RESEARCH ARTICLE | *Sensory Processing*

Electrophysiological responses to lateral shifts are not consistent with opponent-channel processing of interaural level differences

Erol J. Ozmeral,[1] David A. Eddins,[1,2] and Ann Clock Eddins[1]

[1]*Department of Communication Sciences and Disorders, University of South Florida, Tampa, Florida; and* [2]*Department of Chemical and Biomedical Engineering, University of South Florida, Tampa, Florida*

Ozmeral EJ, Eddins DA, Eddins AC. Electrophysiological responses to lateral shifts are not consistent with opponent-channel processing of interaural level differences. *J Neurophysiol* 122: 737–748, 2019. First published June 26, 2019; doi:10.1152/jn.00090.2019.—Cortical encoding of auditory space relies on two major peripheral cues, interaural time difference (ITD) and interaural level difference (ILD) of the sounds arriving at a listener's ears. In much of the precortical auditory pathway, ITD and ILD cues are processed independently, and it is assumed that cue integration is a higher order process. However, there remains debate on how ITDs and ILDs are encoded in the cortex and whether they share a common mechanism. The present study used electroencephalography (EEG) to measure evoked cortical potentials from narrowband noise stimuli with imposed binaural cue changes. Previous studies have similarly tested ITD shifts to demonstrate that neural populations broadly favor one spatial hemifield over the other, which is consistent with an opponent-channel model that computes the relative activity between broadly tuned neural populations. However, it is still a matter of debate whether the same coding scheme applies to ILDs and, if so, whether processing the two binaural cues is distributed across similar regions of the cortex. The results indicate that ITD and ILD cues have similar neural signatures with respect to the monotonic responses to shift magnitude; however, the direction of the shift did not elicit responses equally across cues. Specifically, ITD shifts evoked greater responses for outward than inward shifts, independently of the spatial hemifield of the shift, whereas ILD-shift responses were dependent on the hemifield in which the shift occurred. Active cortical structures showed only minor overlap between responses to cues, suggesting the two are not represented by the same pathway.

NEW & NOTEWORTHY Interaural time differences (ITDs) and interaural level differences (ILDs) are critical to locating auditory sources in the horizontal plane. The higher order perceptual feature of auditory space is thought to be encoded together by these binaural differences, yet evidence of their integration in cortex remains elusive. Although present results show some common effects between the two cues, key differences were observed that are not consistent with an ITD-like opponent-channel process for ILD encoding.

auditory cortex; interaural level differences; spatial hearing

INTRODUCTION

Unlike the visual and tactile sensory systems that topographically represent space in cortex, organization of auditory-source locations are inferred from cues embedded in a tonotopic representation in the primary auditory cortex (Ahveninen et al. 2014; King and Middlebrooks 2010). Human neuroimaging studies and single-cell recordings in non-human primates suggest a coding scheme that depends on wide spatial receptive fields (i.e., hemifield code) rather than narrow tuning of source locations (i.e., place code; Salminen et al. 2009; Werner-Reiss and Groh 2008). In the horizontal plane, the primary auditory spatial cues are the relative arrival times of a sound at the two ears, or interaural time differences (ITDs), and the relative intensity at the two ears, or interaural level differences (ILDs). Peripheral neural processing of ITDs and ILDs have been investigated extensively (for review, see Grothe et al. 2010), yet there still exists an ambiguity in the literature as to how and where the two spatial cues are centrally integrated to form a single auditory space percept.

Evidence for a population rate-based opponent process has been inferred from human neuroimaging studies for ITD coding (Briley et al. 2013; Magezi and Krumbholz 2010; Ozmeral et al. 2016; Salminen et al. 2010, 2015) and for combined ITD and ILD (McLaughlin et al. 2016; Stecker et al. 2015), but it is unclear how the representation of these cues is distributed within and across cortical regions for both static and dynamically changing spatial location. Previous research has shown that evoked potentials for ITD shifts are dependent on the direction of the shift when the shifts occur in a single spatial hemifield (i.e., left or right of center from the listener's perspective). Specifically, shifts away from midline (outward) evoke greater responses than inward shifts, and the reason for this is suspected to confirm population rate-based coding of opposing hemifield channels for ITD representation (Briley et al. 2013; Magezi and Krumbholz 2010; Ozmeral et al. 2016). Similar opponent-channel schemes for ILDs have been inferred as well (McLaughlin et al. 2016; Salminen et al. 2015; Stecker et al. 2015), although they have been based on different stimulus paradigms and recording methodologies. Notwithstanding, some inconsistencies in the literature raise the question of whether ITDs and ILDs are in fact coded by a similar opponent-channel process that reflects a global mechanism for auditory-space coding rather than a specific cue-type representation (Stecker 2018).

Progress has also been made in last two decades investigating whether ITDs and ILDs share a common cortical code (Edmonds and Krumbholz 2014; McLaughlin et al. 2016;

Address for reprint requests and other correspondence: E. J. Ozmeral, Dept. of Communication Sciences and Disorders, University of South Florida, Tampa, FL 33620 (e-mail: eozmeral@usf.edu).

Salminen et al. 2015; Schröger 1996; Tardif et al. 2006; Ungan et al. 2001). Although early work concluded that lateralized stimuli were integrated as early as the brain stem, as measured by the prominent wave V in the auditory brain stem response (Riedel and Kollmeier 2002), the evidence at the cortical level has been elusive. Some have argued that ITD and ILD coding remains independent at least up to the auditory cortex (Tardif et al. 2006; Ungan et al. 2001), yet others suspect that integration occurs more peripherally but with independently maintained information in parallel (Edmonds and Krumbholz 2014). Because ITDs and ILDs elicit similar lateralized percepts, it is plausible that ILDs would not only be coded similarly to ITDs but also share common processing distribution in auditory cortex. Indeed, Salminen et al. (2015) used an adaptation-probe paradigm to demonstrate that cortical responses in left and right cortical hemispheres contralateral to the sound source were sensitive to source location independently of whether the cue was provided by an ITD or ILD, consistent with a location-specific, opponent-channel process. It is not certain whether location-sensitive responses elicited by ITDs or ILDs would be comparable when such cues changed dynamically in the horizontal plane (toward or away from midline).

In the present study, cortical auditory evoked potentials were measured using EEG for binaural stimuli with periodic changes in either ITD or ILD. Previous studies have demonstrated a stereotypic monotonic response for changes in ITD (i.e., increase in magnitude for larger ITD shifts) and direction-specific response patterns (i.e., greater responses to ITDs shifting outward than inward relative to midline), but it is unknown whether the same patterns of responses are seen with changes in ILD. Moreover, it is not known whether the strength of the activity is distributed across the cortex in shared regions (i.e., primary auditory cortex). Demonstration of like responses between ITD and ILD shifts would provide additional support for a common coding scheme between them and possibly for the perceptual change itself, but deviations in the elicited responses would implicate a continued, partially independent representation in early cortical areas.

The primary goal of the study was to evaluate whether listeners exhibit comparable EEG response activity to changes in perceived sound lateralization due to ITDs alone and ILDs alone. In earlier work from the present authors, a cohort of young, normal-hearing listeners were tested on a similar paradigm using only ITDs to induced changes in perceived lateralization of a noise stimulus (Ozmeral et al. 2016). That work focused on potential explanations for temporal processing declines with age, and it followed procedures by Magezi and Krumbholz (2010). Magezi and Krumbholz measured electrophysiological responses to a low pass-filtered noise burst that abruptly changed ITD after an adaptation period. Perceptually, the probe stimulus either increased or decreased in laterality in the same hemifield relative to the initial ITD. Responses to the ITD change were consistent with predictions based on a nontopographical representation of ITD coding in which increased lateralization produced significantly larger responses than decreased lateralization. This general outcome has been replicated a number of times both over headphones (Ozmeral et al. 2016) and in the free field using low-frequency stimuli associated with prominent ITD cues (Briley et al. 2013). In studies by both Ozmeral et al. (2016) and Magezi and Krumbholz (2010), younger listeners showed significantly higher magni-

tudes and shorter latencies in the cortical responses to ITD shifts away from midline (outward) relative to shifts toward midline (inward). As a window into the potential shared or disjoined processing of the two binaural cues, the present study tested whether ILD shifts would evoke the same pattern of cortical behavior as previously seen with ITDs.

MATERIALS AND METHODS

Participants. Ten young, normal-hearing participants (6 women and 4 men), aged 21–27 yr, participated in the experiment. Pure-tone air and bone conduction thresholds were within normal limits [≤20 dB hearing loss (HL)] at octave frequencies from 250 to 8,000 Hz (ANSI 2010). Participants were excluded if they reported a history of neurological dysfunction, middle ear disease, or any ear surgery. The Montreal Cognitive Assessment (MoCA) was administered to all participants to screen for cognitive impairment, and all listeners scored at least 26 or higher (Nasreddine et al. 2005). Listeners provided written informed consent and were compensated for their participation as approved by the Institutional Review Board of the University of South Florida.

Stimuli. Acoustic stimuli were narrowband noise bursts (500–750 Hz) presented binaurally at a fixed combined level of 80 dB SPL. An ILD and ITD was imposed on stimuli for dichotic conditions. The possible ITDs included ±500, ±250, and 0 μs, and possible ILDs included ±20, ±10, and 0 dB, in which a negative (or positive) value indicates leading in the left (or right) ear or higher intensity in the left (or right) ear, respectively. For ITD-shift conditions, ILD was held constant at 0 dB, and for ILD-shift conditions, ITD was held constant at 0 μs. Signals were generated in MATLAB at a 24,414-Hz sampling rate (41-μs resolution) and gated on and off with 10-ms cosine ramps. Stimulus durations were specific to the testing session procedures (see below).

Experimental design: behavioral test. Participants performed a behavioral task to provide individual data on the perceived relative lateralization between the ITD and ILD cues presented in the EEG experiment. Stimulus generation, presentation, and response collection were controlled via SykofizX software (Tucker-Davis Technologies, Alachua, FL) and presented over ER-3A insert earphones (Etymotic Research, Elk Grove Village, IL) in a single-walled, sound-treated booth via an RZ6 multi-input/output processor (Tucker-Davis Technologies). Two conditions were tested: *1)* ITD target with ILD probe and *2)* ILD target with ITD probe. On each trial, listeners received a 400-ms target interval followed by a 400-ms probe interval (inter stimulus interval of 500 ms). The target ITDs and ILDs were selected from those used in the EEG session, and each was tested 10 times in a random order. The initial ILD or ITD of the probe was chosen to be perceived more to the left or more to the right of the target on the basis of pilot testing, and each initial probe cue was tested five times. Listeners indicated by button press on a graphical user interface which direction ("Left" or "Right") would move the probe's intracranial position closer to that of the target. For the ILD probe, a press of the Left (Right) button increased the intensity in the left (right) ear by 1 dB and decreased the intensity in the right (left) ear by 1 dB for an overall shift in ILD by 2 dB in favor of the left (right) ear. For the ITD probe, a press of the Left (Right) button increased the temporal lead of the left (right) ear by 25 μs. Following the subject's selection, the trial restarted with the proper update to the probe only. When the subject was confident that the target and probe matched in their intracranial position, he or she pressed a button labeled "Next." Total behavioral testing time for each participant was ~1.5 h, which was completed on a separate day before the EEG sessions.

Experimental design: electrophysiology test. Listeners were seated in a double-walled, sound-treated booth (Acoustic Systems, Cedar Park, TX) and, throughout testing, were allowed to watch a silent captioned video from an online streaming service. Stimuli were
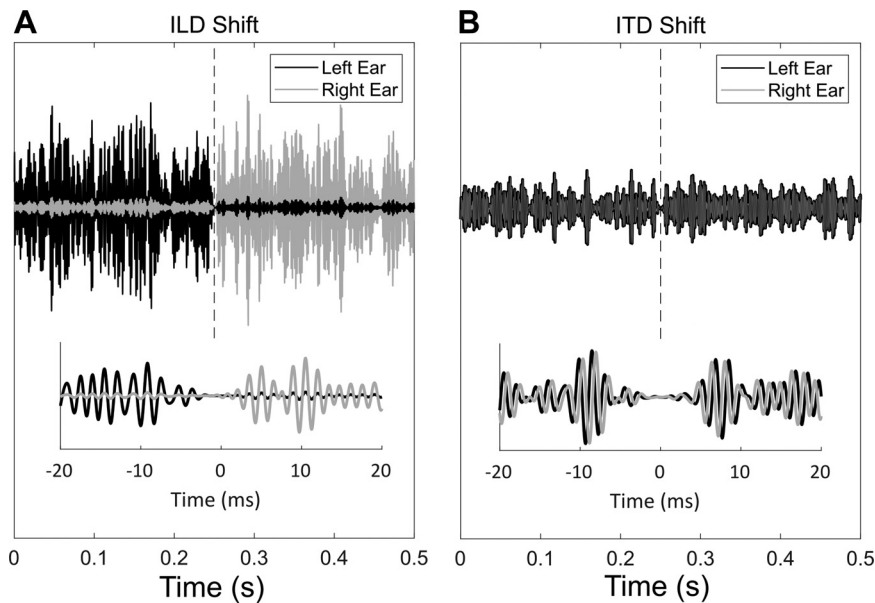
Fig. 1. Sound pressure waveform of the interaural level difference (ILD; *A*) and interaural time difference (ITD; *B*) conditions. Each waveform is shown for 0.25 s before and after a cue shift, as well as for a 40-ms window around the cue transition in the *inset*. The left ear receives the signal represented by a black line, and the right ear receives the signal represented by the gray line.

presented over ER-2 insert earphones (Etymotic Research) via an RZ6 multi-I/O processor (Tucker-Davis Technologies). Listeners were instructed to remain as still as possible and to ignore the auditory stimuli during the two recording sessions. Each of the two recording sessions consisted of four blocks, in which each block consisted of 800 uninterrupted trials with a duration of 1,600 ms per trial. The order of the eight total blocks was randomly assigned across participants. Stimuli presented per trial were as described above with a pseudorandomly imposed ITD (in μs) or ILD (in dB) depending on the block. Each 1,600-ms interval was created by first generating the binaural stimulus with a duration of 1,620 ms including on and offset ramps, and then concatenating with the next interval with 10-ms overlap. Figure 1 shows the stimulus time waveforms for a 0.5-s sample centered at the transition from −20 to +20 dB ILD (*A*) and from −500 to +500 μs ITD (*B*). Insets in each panel show a smaller time window to highlight the cue transition. The onset trigger of each trial within a block represented a pair of ITDs or ILDs, also referred to as a "shift pair." That is, the presentation of a binaural stimulus for 1,600 ms that has an abrupt change in that binaural cue consists of a preshift adapter and a postshift probe. Each block was designed to include 32 presentations of each possible shift pair. In each cue condition (ITD or ILD), there were five lateralization possibilities and thus 25 lateralization shift pairs (e.g., +500/−250 μs, 0/−500 μs, +250/+250 μs, etc.), including shift pairs between unchanged cues (e.g., −10/−10 dB). Note that the postshift probe for one pair was the subsequent preshift adapter for the subsequent pair. Across the full experiment (4 blocks per binaural cue), each of the 25 pairs was presented 128 times. Figure 2 provides a usable matrix to visualize the magnitude (*A*) and direction (*B*) of the 25 switch pairs presented in each binaural condition, where the step size (*X*) was either 250-μs

ITD or 10-dB ILD. In 12 of the 25 shift pairs, there was either a perception of an outward shift (away from midline; e.g., −250/−500 μs) or an inward shift (toward midline; e.g., +20/0 dB) in a single spatial hemifield (left or right of midline). In five of the shift pairs, no cue change was made, and these conditions served as a control (diagonal from *top left* to *bottom right* in Fig. 2). The remaining eight pairs consisted of a crossing from one hemifield to the other (e.g., −10/+10 dB). Total testing time, including frequent breaks between blocks, was ~4 h over 2 testing days.

EEG recording and data analysis. Continuous EEG was recorded using a Waveguard (ANT Neuro, Enschede, The Netherlands) elastic cap with 64 sintered Ag-AgCl electrodes (International 10–20 electrode system), and additional bipolar eye electrodes were placed on the supra- and infraorbital ridges of the left eye to monitor blinks during the testing. All electrode impedances were <10 kΩ, and the recordings were referenced to the mean across channels with digitization at 512 Hz and 24-bit precision. Ground was located at the central forehead (AFz). Recordings were made through asalab acquisition software (ANT Neuro), and stimulus and triggering were controlled using custom MATLAB scripts (The MathWorks, Natick, MA).

Recordings were processed offline using the software suite Brainstorm (Tadel et al. 2011), running within MATLAB. Preprocessing of raw recordings consisted of *1*) bandpass filtering between 0.1 and 100 Hz (slope of 48 dB/octave), *2*) notch filtering at 60 Hz and harmonics, *3*) automatic detection of eye blinks based on the electro-oculogram electrodes (Tadel et al. 2011), *4*) re-referencing to the average and artifact removal based on signal-source projections (SSP; Gramfort et al. 2014; Uusitalo and Ilmoniemi 1997). The SSP approach is very similar to an independent component analysis that performs a spatial
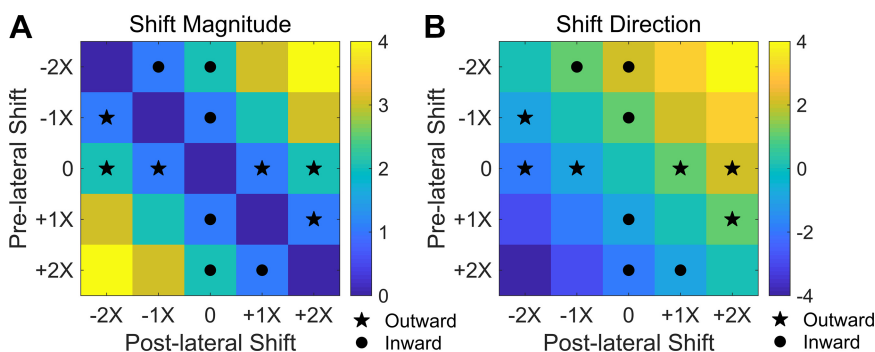

Fig. 2. A reference matrix for the cue transitions with respect to the intralateral position before (rows) and after (columns) the cue shift. The cue step sizes (*X*) were 250-μs interaural time difference shifts and 10-dB interaural level difference shifts. Shifts along the downward diagonal were catch trials in which no shift was made; thus stimuli were presented at the same location for twice as long. *A*: each box of the matrix indicates the magnitude of the shift, as represented by the color map at *right*. *B*: each box of the matrix indicates the direction of the shift with positive values indicating rightward shifts and negative values indicating leftward shifts. Conditions that were considered as "outward" are marked by stars, and those considered as "inward" are marked by circles.

decomposition of the signals for the purposes of identifying the topographies of an idiosyncratic event, such as an eye blink. Because these events are very reproducible and occur at the same location, this analysis can use their spatial topographies to remove their contribution from the recording while preserving contributions from other generators. Following preprocessing stages, each of the continuous recordings was epoched by trigger type, corresponding to each of the shift pairs. Trigger labels were applied at time of measurement in which both the pre- and postshift cues were coded in the label. For both ITD and ILD conditions, there were five possible lateralizations, and thus 25 possible pre- and postshift combinations including the no-shift condition (see Fig. 2). All epochs of a single cue-shift combination were then averaged following removal of direct current (DC) offset and linear drift. In many cases, shift combinations had commonalities with other shift combinations along one or more dimensions, and in such cases, the averages across these common shift combinations were also performed. These analyses were designed to explore whether differences in response magnitude were simply dependent on the size of the lateralization change and independent of cue type. As an example, the spatial hemifield of the perceived lateralization was not always analyzed independently, and thus an epoch representing an ILD shift from 0 to +10 dB was not distinguished from an epoch representing a shift from −10 to −20 dB. In this example, the magnitude of the shift was 10 dB, and neither the hemifield of the shift nor the direction were parsed. In other analyses, epochs were considered more independently and indicated as such. Once individual data had been fully processed, grand averages and SD were computed across all subject data for each individual cue shift as well as for certain groupings. Groupings included those based on *1*) magnitude of shift (collapsed across directions and spatial hemifields) and *2*) direction of shift (collapsed across varying shift magnitudes).

Statistical analysis: auditory event-related potentials. A number of the present analyses rely on the auditory event-related potential (ERP; Luck 2014) in the measured EEG waveforms. An ERP traditionally consists of a triphasic waveform with peak magnitudes roughly 50, 100, and 200 ms following a physical change to the auditory stimulus (e.g., Figs. 4–6). These peaks, also referred to as the P1, N1, and P2 components, respectively, are robust to stimulus changes in frequency (Kohn et al. 1978), intensity (Picton et al. 1976), and/or space (McEvoy et al. 1990) in young, normal-hearing listeners. In the present study, the larger N1 and P2 components were specifically analyzed. Figures 4–6 include average ERPs at the vertex electrode (Cz), which are representative of the evoked response to cue shifts; however, to capture the totality of synchronous neural sources, the global field power (GFP; Skrandies 1990) was computed across all 64 scalp electrodes. For individual averaged epochs, peak magnitudes of the GFP were extracted by computing the maximum negativity or positivity in a certain latency window (N1: 80–160 ms; P2: 180–260 ms following cue shift). Latency windows were chosen by first finding the mean peak latency per component and then, at the individual level, extracting the peak GFP within an 80-ms window around that mean peak. The effects of shift size, direction of shift, and spatial hemifield

on ERPs were tested by analysis of variance (ANOVA) on the magnitude of the GFP.

Statistical analysis: cortical source localization. Source-localized waveforms were estimated using standardized low-resolution brain electromagnetic tomography (sLORETA; Pascual-Marqui 2002). The sLORETA technique is built into the Brainstorm analysis suite (Tadel et al. 2011). This technique estimates a single solution to the inverse problem (Grech et al. 2008) for determining the cerebral source of neural generation observed at the scalp with EEG. Head volume is calculated using the boundary element method (OpenMEEG; Gramfort et al. 2010; Kybic et al. 2005), which assumes isotropic tissue conductivities. A standardized current density (in pA·m) is calculated at each of 15,000 voxels in the gray matter and the hippocampus of the Collin27 stereotaxic registration model (Holmes et al. 1998). Dipoles were contained to normal orientations relative to cortex. The Destrieux atlas (Destrieux et al. 2010) was then used to parse the cortex into regions of interest (ROIs). To analyze activity across ROIs, the mean waveforms within an ROI was extracted. As with the scalp electrode analyses, the individual peak magnitudes were identified at the N1 and P2 latencies using an 80-ms window around the average peak across conditions. Resulting measures were organized by binaural cue type, shift direction, and the spatial hemifield in which the shift occurred (left or right) and were then submitted to ANOVA statistical testing.

RESULTS

Comparison between intracranial position of ILD and ITD targets. Behavioral data were used mostly to verify the perceived intracranial differences between tested ILDs and ITDs in the electrophysiological testing. As such, it was expected that in both conditions, there would be a linear relationship between the lateralization of the target cue and the probe cue. This was especially important for the chosen set of ILDs because of the low-frequency characteristics of the noise stimuli, which would imply poor available ILD cues in a natural environment (Blauert 1997). To compare across target-cue conditions, subject data were first normalized by their *z* transform. Next, data were submitted to a linear regression model to determine parameters that best predicted the probes. Mean (SD) normalized data are shown in Fig. 3 with the respective linear fit to the mean, where *y* is the expected probe *z* score for *x* steps away from midline. Results show that lateralization of a target ITD (Fig. 3*A*) or ILD (Fig. 3*B*) was linearly matched with the other cue. Variance among the 10 participants appeared higher when an ILD probe was matched to a target ITD (Fig. 3*A*) relative to the opposite case. Nevertheless, the participants showed discrete perceptual differences among the different targets for a given cue type, indicated by significant
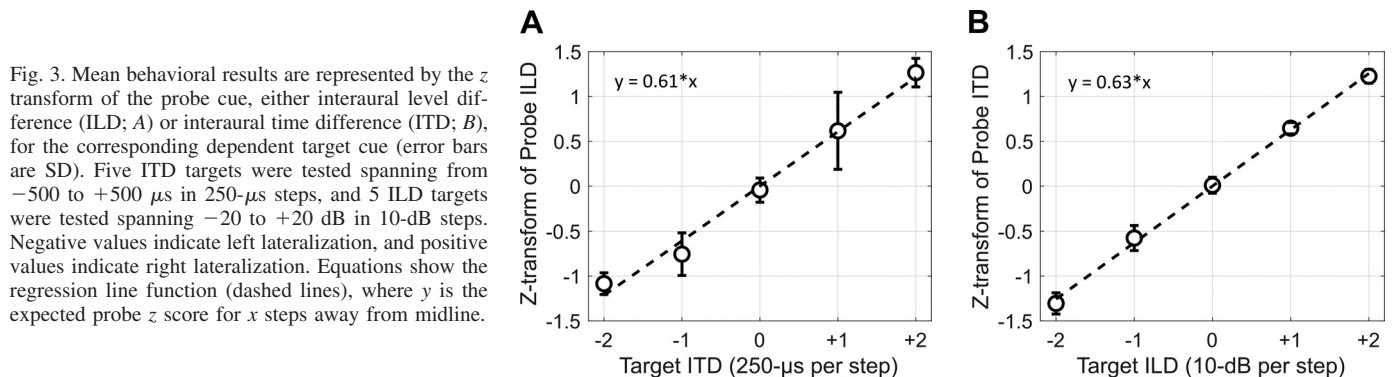
Fig. 3. Mean behavioral results are represented by the *z* transform of the probe cue, either interaural level difference (ILD; *A*) or interaural time difference (ITD; *B*), for the corresponding dependent target cue (error bars are SD). Five ITD targets were tested spanning from −500 to +500 µs in 250-µs steps, and 5 ILD targets were tested spanning −20 to +20 dB in 10-dB steps. Negative values indicate left lateralization, and positive values indicate right lateralization. Equations show the regression line function (dashed lines), where *y* is the expected probe *z* score for *x* steps away from midline.

A
$y = 0.61 * x$

Z-transform of Probe ILD
Target ITD (250-µs per step)

B
$y = 0.63 * x$

Z-transform of Probe ITD
Target ILD (10-dB per step)

linear, within-subject contrasts for a repeated-measures ANOVA with one factor [5 target cues; ITD: $F(1,9) = 43.7$, $P < 0.001$; ILD: $F(1,9) = 432$, $P < 0.001$]. The significant linear relationship suggests that changes between two targets within a cue type would evoke a perceptual intracranial position change, and the nearly equivalent regression slopes suggest that direct comparisons across cue types are substantiated. That is, a shift from an ILD of -20 to -10 dB can be assumed to evoke a similar perceived magnitude of change in intracranial position as an ITD shift of -500 to -250 μs.

Effect of shift size on the elicited ERP responses. The behavioral data confirmed the perceptual similarity among the tested cue shifts, and the electrophysiology was consistent with this perceptual similarity. Scalp electrode measures were initially epoched and averaged by trial type, which was unique for each cue, shift direction, and shift size (see Fig. 2). The following sections collapse over a number of similar trial types, specifically by shift magnitude and direction.
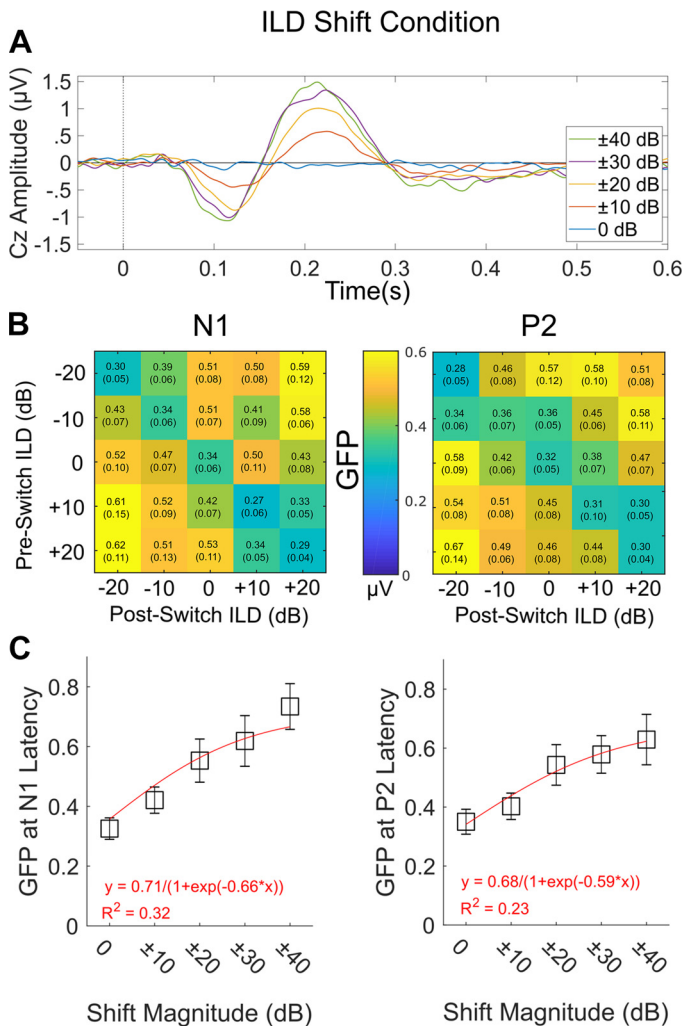
Fig. 4. *A*: vertex (Cz) responses as a function of interaural level difference (ILD)-shift magnitude. *B*: each matrix represents the global field power (GFP; in μV) recorded at the 2 late-latency components, N1 (*left*) and P2 (*right*), for ILD shifts. Refer to Fig. 2 for a reference matrix regarding the magnitude of the shifts. Values are means (SE) across subjects. *C*: individual means were fit to a logistic function. The fitted model, *y*, is presented by the red curve and equation.
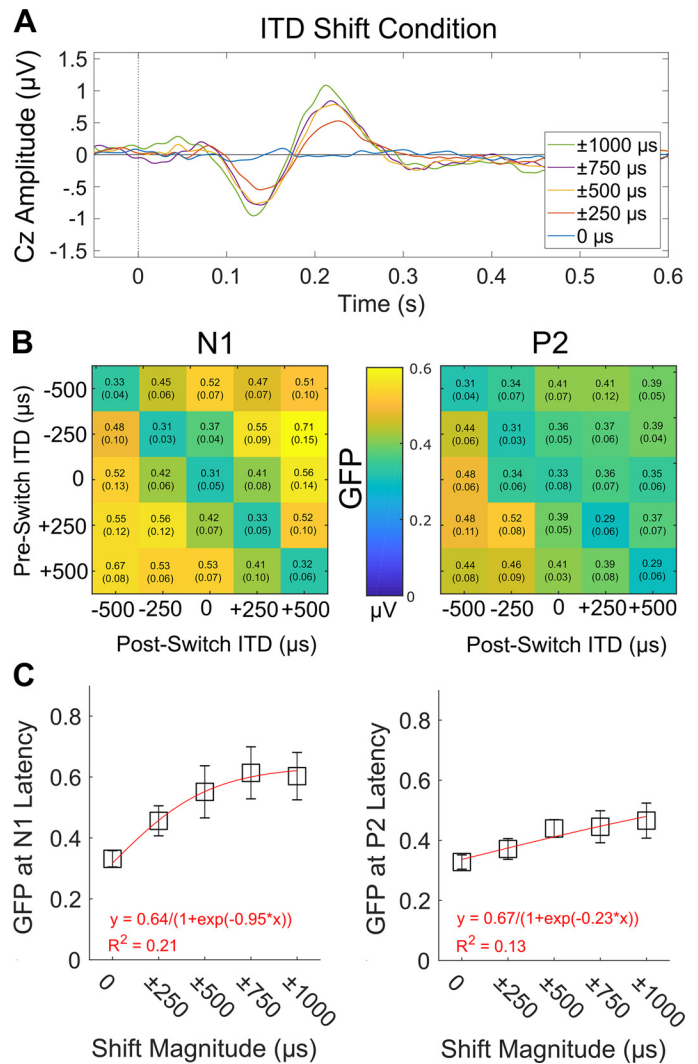
Fig. 5. *A*: vertex (Cz) responses as a function of interaural time difference (ITD)-shift magnitude. *B*: each matrix represents the global field power (GFP; in μV) recorded at the 2 late-latency components, N1 (*left*) and P2 (*right*), for ITD shifts. Refer to Fig. 2 for a reference matrix regarding the magnitude of the shifts. Values are means (SE) across subjects. *C*: individual means were fit to a logistic function. The fitted model, *y*, is presented by the red curve and equation.

Figures 4*A* and 5*A* display the average scalp recordings at vertex (Cz) for the ILD and ITD conditions, respectively. The shift in ITD or ILD was expected to evoke an ERP that was dependent on the magnitude and direction of the shift (Ozmeral et al. 2016). For the present analysis, data were collapsed across equal-sized shifts in opposite directions so that, for example, no distinction was made between the largest ILD shift from -20 to $+20$ dB (left to right hemifield) and $+20$ to -20 dB (right to left hemifield). The morphology of the ERP following the binaural cue shift (*time 0*) had two prominent components at latencies of around 110 and 220 ms, corresponding to the N1 and P2 components, respectively. For both the ILD (Fig. 4*A*) and ITD (Fig. 5*A*) conditions, as the degree of shift magnitude increased from 0 dB or 0 μs, respectively, the magnitude of the ERP components increased monotonically. For example, the evoked response at the vertex electrode for a change in ILD of ±10 dB had a maximum peak of roughly 0.5 μV, whereas a change in ILD of ±40 dB had a
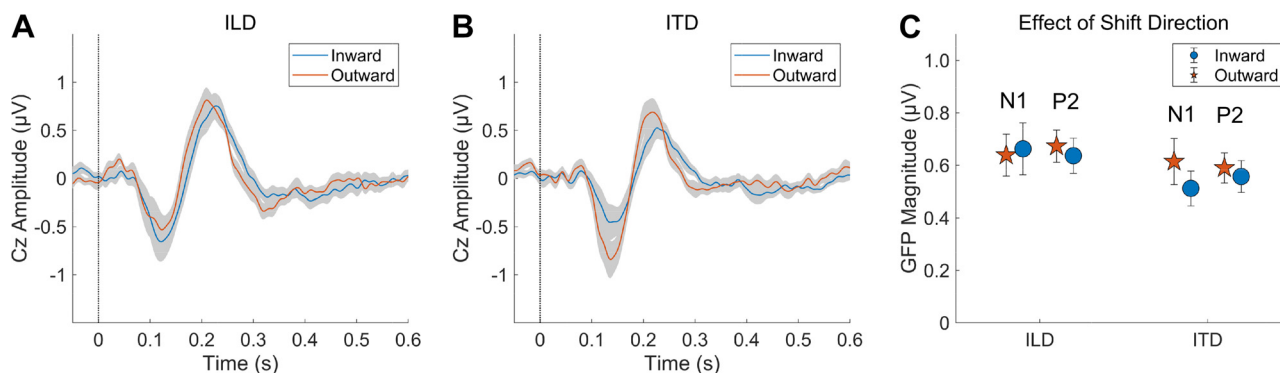
Fig. 6. Vertex (Cz) responses as a function of cue-shift direction. Data were condensed across all inward (blue) and all outward (red) shifts (see Fig. 2 for reference). *A*: elicited responses are shown to be comparable for interaural level difference (ILD) shifts. *B*: elicited responses are shown to be larger for outward interaural time difference (ITD) shifts. *C*: mean global field power (GFP) of the N1 and P2 latencies for each cue is shown, with blue circles indicating inward conditions and red stars indicating outward conditions. Error bars are SE.

maximum peak of nearly 1.5 μV in the P2 component, a threefold difference. Similarly, a change in ITD of $\pm$1,000 μs evoked a greater response than that of $\pm$250 μs, by about twofold.

To capture the neural synchrony associated with the spatial change detection, GFP was analyzed at the N1 and P2 deflections. Figure 4*B* (ILD) and Fig. 5*B* (ITD) show the mean GFP per trial type for the N1 and P2 latencies. It is clear that a graded response occurs for both ITD and ILD shifts depending on the magnitude of the shift (largest shifts are represented in *top right* or *bottom left* corners of Figs. 4*B* and 5*B*; also see Fig. 2). Whereas both cues appear to have comparable signatures at the N1 latency, there appears to be greater overall activity at P2 for ILD shifts relative to ITD shifts, perhaps indicating higher order processes for the ILD shifts. The GFP measures at N1 and P2 latencies were submitted to a two-way mixed-model ANOVA with subjects as a random factor and fixed factors of cue type (ITD or ILD) and shift size (0, 1*x*, 2*x*, 3*x*, or 4*x*, where *x* indicates the cue parameter). The direction of the shift was not considered, because the primary question in this case is whether the magnitude of a shift has an effect on the measured ERP. At the N1 latency, no difference was found between cue types, and shift magnitude was indeed a significant factor [$F_{(4,36)} = 35.7$, $P < 0.001$, $\eta_p^2 = 0.80$]. There was also a significant interaction between cue and shift magnitude [$F_{(4,36)} = 5.7$, $P = 0.001$, $\eta_p^2 = 0.39$], consistent with the greater effect of shift magnitude with ILD stimuli than ITD stimuli. At the P2 latency, there were significant effects of both shift size and cue [$F_{(4,36)} = 46.2$, $P < 0.001$, $\eta_p^2 = 0.84$ and $F_{(1,9)} = 10.9$, $P < 0.01$, $\eta_p^2 = 0.55$, respectively], as well as the interaction [$F_{(4,36)} = 4.5$, $P < 0.005$, $\eta_p^2 = 0.33$]. The interaction was likely explained again by the greater effect of shift magnitude with ILD stimuli relative to ITD stimuli. To more fully characterize the relationship between shift magnitude and ERP activity, a post hoc model was applied to the individual GFP data averaged across shift magnitudes. Figures 4*C* and 5*C* present the mean GFP data as a function of shift magnitude. The corresponding fitted model and model equations are also given. A sigmoidal model was chosen because of an observed compression in the overall activity as shift magnitude reached the extreme shifts tested. In general, the mean GFP was captured by models with fitted parameters, except for the ITD P2 measures, which had a much shallower slope

parameter. To summarize, the present observations confirm that the magnitude of a binaural shift is monotonically related to the amplitude of the elicited response and that the responses to the two cues are mostly similar with respect to shift magnitude, at least at the earlier N1 neural component.

Effect of shift direction in a single spatial hemifield. Figure 6 shows the scalp-level EEG averaged across all subjects for the two possible shift directions per cue type as measured by the vertex electrode. The vertex response is displayed collapsed across spatial hemifields and equivalent shift directions such that, for example, no distinction was made between outward shifts from +10 to +20 dB in the right hemifield and from 0 to −20 dB in the left hemifield (both falling under "outward" regardless of shift size). As was the case for shift magnitude, shift direction in a single hemifield (either outward or inward) evoked an ERP with two prominent components at latencies of around 110 and 220 ms, corresponding to the N1 and P2 components, respectively. At the vertex, there appears to be a dominant effect of outward shifting ITDs relative to inward shifts (Fig. 6*B*), but no such difference emerges with ILD stimuli (Fig. 6*A*). To take into account all electrode channels, the individual GFP measures were submitted to a two-way repeated-measures ANOVA with factors of cue type (ITD and ILD) and shift direction (outward or inward). The primary question was whether outward shifts evoked larger responses in either cue type as has been previously shown for ITD shifts (e.g., Ozmeral et al. 2016). Figure 6*C* presents the mean data for each cue type at the N1 and P2 latencies. For the N1 component, there was a significant main effect of cue type [$F_{(1,9)} = 6.9$, $P < 0.05$, $\eta_p^2 = 0.43$] as well as a significant interaction between cue type and shift direction [$F_{(1,9)} = 5.5$, $P < 0.05$, $\eta_p^2 = 0.38$]. The interaction is explained by a greater response to the outward than the inward direction for ITD shifts, but for ILD shifts, no such difference was observed at the N1 latency. For the P2 component, no interactions were significant; however, overall cortical responses in the ILD-shift conditions were found to be significantly larger than the ITD-shift conditions [$F_{(1,9)} = 15.5$, $P < 0.005$, $\eta_p^2 = 0.63$], and there was a significant main effect of shift direction, with outward shifts evoking significantly larger responses than inward shifts [$F_{(1,9)} = 6.5$, $P < 0.05$, $\eta_p^2 = 0.42$]. To summarize, the present observations confirm a shift-direction effect for both binaural cues at the later ERP component latency (P2)

but not at the early component latency (N1), which only showed a shift-direction effect for ITD shifts.

Hemispheric distribution of activity from cue shifts. The estimated location of neural generators was assessed for the ERPs analyzed above. In particular, it was of interest to determine the hemispheric distribution of activity in response to lateralized shifts within each hemisphere due to previous accounts for ITD-shift coding and their implications for population rate-based models (Magezi and Krumbholz 2010). An atlas was used to parse the cortex into ROIs that included not only auditory-associated areas but also non-auditory-associated areas (Destrieux et al. 2010). This allowed for comparisons between binaural cues across all cortical areas, for example, areas that are associated with encoding spatial percepts (Zatorre et al. 2002). Figure 7 shows the resulting waveforms from the left and right auditory cortices, which were derived from the mean across three ROIs (anterior transverse temporal gyrus of Heschl, temporal plane of the superior temporal gyrus, and transverse temporal sulcus) that encompass the primary auditory cortex (A1). Line types indicate outward and inward shifts, and mean topographies are displayed below each waveform at the peak N1 and P2 latencies. Figure 7, *A* and *B*, show the ILD-shift conditions, and Fig. 7, *C* and *D*, show the ITD-shift conditions. Figure 7, *A* and *C*, represent shifts in the left spatial hemifield, whereas Fig. 7, *B* and *D*, represent shifts in the right spatial hemifield.

Together, Fig. 7, *A–D*, demonstrate both similarities and differences between ITD and ILD representation. First, as was shown earlier at vertex in Fig. 6*B* and in the GFP in Fig. 6*C*, outward shifts evoked larger responses than inward shifts for ITDs at N1 latencies. Figure 7, *C* and *D*, shows that this is likely driven by the contralateral auditory cortex relative to the hemifield of the ITD shift. That is, when the outward ITD shift was in the left spatial hemifield (Fig. 7*C*), there was a prominent N1 response in right A1, and when the outward ITD shift was in the right spatial hemifield (Fig. 7*D*), there was a prominent N1 response in left A1. On the contrary, elicited responses to ILD shifts previously showed no discrepancy between inward and outward directions in the N1 component (see Fig. 6*A*), but Fig. 7, *A* and *B*, clearly shows prominent effects of direction, albeit opposite effects depending on the spatial hemifield of the shift. According to this source analysis, ILD shifts evoke a large N1 response in right A1 response to outward shifts when the shift is in the left hemifield, as was the case for ITD shifts; however, when ILD shifts were in the right spatial hemifield, the largest evoked responses occurred at N1 when the shift direction was toward midline (i.e., inward). Whereas the contralateral hemisphere appears to follow an expected outward dominance, this ipsilateral bias toward inward ILD shift is particularly dissimilar from what was seen for ITD-shift responses. This observed difference is also the likely reason that no direction effect was seen when only the
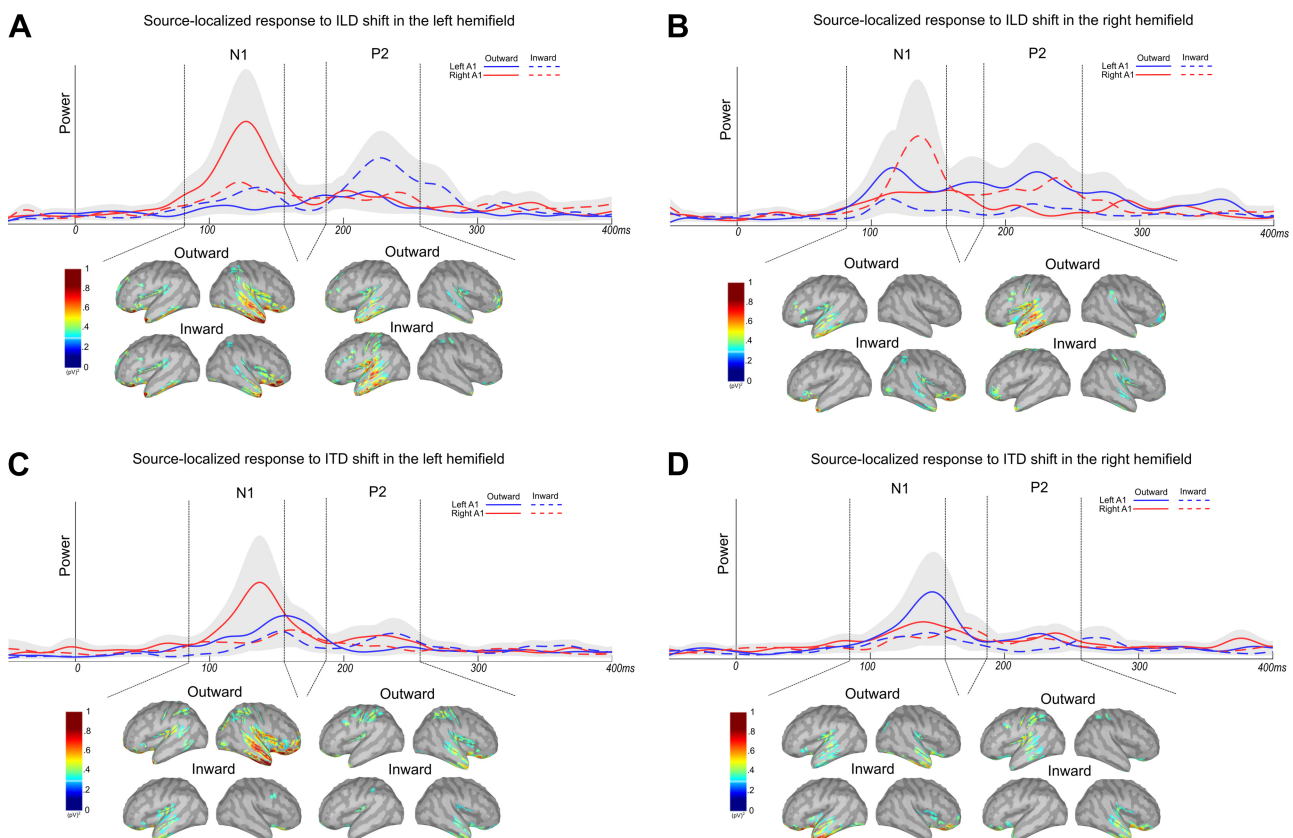

Fig. 7. Waveforms from the left and right primary auditory cortex (A1; blue and red lines, respectively), which were derived from the mean across 3 regions of interest (anterior transverse temporal gyrus of Heschl, temporal plane of the superior temporal gyrus, and transverse temporal sulcus) that make up A1. Line types indicate outward (solid) and inward shifts (dashed), and representative mean topographies are displayed below each waveform at the N1 and P2 latencies. The N1 and P2 magnitudes were found within the range depicted by the dotted lines on an individual basis. *A* and *B*: interaural level difference (ILD)-shift conditions. *C* and *D*: interaural time difference (ITD)-shift conditions. *A* and *C* represent shifts in the left spatial hemifield, whereas *B* and *D* represent shifts in the right spatial hemifield. Shaded regions represent SE.

GFP or vertex activity was viewed (Fig. 6, *A* and *C*). Finally, there was apparent later activity at the P2 latency for ILD shifts and lack thereof for ITD shifts, indicating a potentially higher order processing for ILDs that is lacking for ITDs, at least at the level of the primary auditory cortex.

Because A1 does not appear to be the only area that differed across cues, the waveforms across all ROIs were analyzed. The N1 and P2 peak magnitudes were extracted for each subject at each ROI and submitted to a four-way mixed-model ANOVA with subjects as a random effect and fixed effects of shift direction, shift hemifield, and cortical hemisphere. The results indicated that significant main effects and interactions were exclusive to the magnitudes at the N1 latency. In many cases there were significant main effects of either spatial hemifield or cortical hemisphere, as well as the interactions between the two. Often these were driven by expected greater contralateral activity for a given spatial stimulus (von Kriegstein et al. 2008)

or a generally larger activity level in the right hemisphere (Griffiths et al. 1998; Zatorre et al. 1999). Because of a particular interest in the effect of direction (and potential interactions with cortical hemisphere or spatial hemifield), Table 1 only reports each of the main effects and interactions with direction for the tested ROIs (numbers correspond to the atlas in Destrieux et al. 2010) that were significant ($\alpha = 0.05$). Post hoc *t*-tests indicate which direction had greater activity (positive values for outward greater than inward shifts). Only the opercular part of the inferior frontal gyrus (index 12) was a shared region of effect between the two cues. Figure 8 displays the topographical ROIs listed in Table 1 for both ILDs (*A*) and ITDs (*B*).

From Table 1, it is clear that there are considerable differences in the effect of shift direction between the two cues such that ITD shifts tended to show outward shifts with greater activity than inward shifts, whereas ILD changes often had an

Table 1. *Topographical regions of interest*

Cue	Destrieux Index	Anatomical Reference	Effect	*F*	*P*	Post Hoc (*t*)	*P*
ILD	12	Opercular part of inferior frontal gyrus	Hemisphere × hemifield × direction	6.1	0.038		
	14	Triangular part of inferior frontal gyrus	Hemifield × direction	6.9	0.031		
	16	Superior frontal gyrus	Hemisphere × direction	5.7	0.045		
	17	Long insular gyrus and central sulcus of insula	Hemisphere × direction	6.4	0.035		
	20	Superior occipital gyrus	Direction	5.6	0.045	−1.7	0.089
	45	Central sulcus	Hemifield × direction	5.8	0.043		
	46	Marginal branch (or part) of cingulate sulcus	Hemisphere × hemifield × direction	5.8	0.042		
	51	Posterior transverse collateral sulcus	Hemisphere × hemifield × direction	12.1	0.008		
	67	Postcentral sulcus	Hemisphere × hemifield × direction	5.5	0.048		
	73	Superior temporal sulcus	Hemisphere × hemifield × direction	7.1	0.029		
	74	Transverse temporal sulcus	Hemifield × direction	8.4	0.020		
ITD	12	Opercular part of inferior frontal gyrus	Direction	8.2	0.021	2.3	0.022
	13	Orbital part of inferior frontal gyrus	Hemisphere × direction	7.1	0.029		
	18	Short insular gyri	Direction	6.6	0.033	−1.5	0.142
	34	Lateral aspect of the superior temporal gyrus	Hemifield × direction	8.4	0.020		
	39	Horizontal ramus of anterior segment of lateral sulcus	Direction	7.3	0.027	1.2	0.232
	40	Vertical ramus of anterior segment of lateral sulcus	Hemisphere × direction	7.2	0.028		
	40	Vertical ramus of anterior segment of lateral sulcus	Direction	6.7	0.032	1.8	0.079
	44	Calcarine sulcus	Direction	5.8	0.043	1.1	0.265
	44	Calcarine sulcus	Hemisphere × hemifield × direction	6.3	0.036		
	58	Superior occipital sulcus and transverse occipital sulcus	Direction	5.4	0.048	1.0	0.304
	60	Lateral occipitotemporal sulcus	Direction	6.2	0.037	1.9	0.057
	63	Medial orbital sulcus	Direction	5.6	0.046	1.6	0.110

ILD, interaural level difference; ITD, interaural time difference.
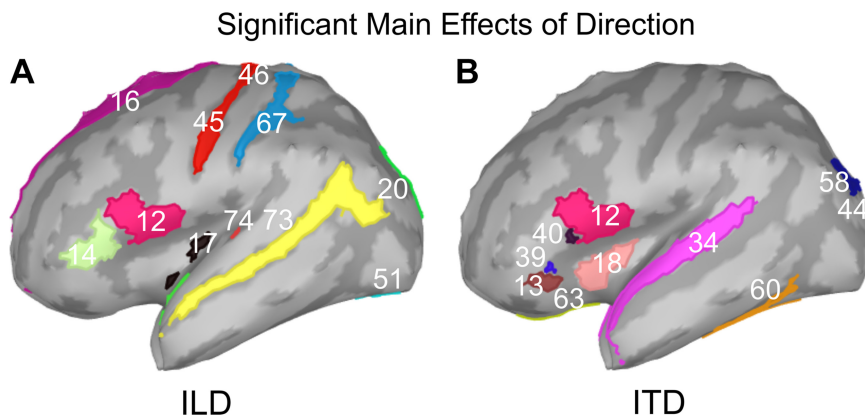
Significant Main Effects of Direction

Fig. 8. Topographical regions of interest (ROIs) as listed in Table 1 for both interaural level difference (ILD; *A*) and interaural time difference (ITD; *B*). The ROIs indicate where main effects of shift direction were identified in the analyses described in the text.

interaction between spatial hemifield and direction. A representative case of the latter in the primary auditory cortex is shown in Fig. 7 in which outward shifts evoked larger amplitudes than inward shifts when the signal was presented with ILDs favoring the left hemifield (*A*), yet inward shifts were greater than outward shifts when the signal was spatially to the right (*B*). That is, ILD and ITD shifts appear to share a common cortical response when the stimuli are in the left hemifield and processed contralaterally, but they show opposing responses when the stimuli are in the right hemifield.

DISCUSSION

The aim of this study was to consider whether azimuthal localization cues, ITDs and ILDs, share a common neural code—specifically, a population rate-based opponent-channel process that has already been implicated in ITD coding (Briley et al. 2013; Magezi and Krumbholz 2010; Salminen et al. 2010) and has been inferred with ILD coding (Altmann et al. 2014; Higgins et al. 2017; McLaughlin et al. 2016). Previous investigations have reported that a rapid increase in ITD (outward lateralization relative to midline) evokes a stronger cortical EEG response than a rapid decrease in ITD (inward lateralization). Within an adapter-probe construct, as in the present study, this has been interpreted as evidence for neural populations that have strong preference for one ITD spatial hemifield over the other (Magezi and Krumbholz 2010). The relative rates between these broad neural populations are believed to encode ITDs rather than a place code made up of many narrowly tuned neural populations. Moreover, both EEG and functional MRI studies have indicated that multiple broad channels exist across cortical hemispheres such that unilateral lesions to the left auditory cortex do not impair spatial hearing (Griffiths et al. 1997; Zatorre and Penhune 2001), although there is some indication that binaural cues are disproportionately encoded in contralateral hemispheres (Stecker et al. 2015; von Kriegstein et al. 2008). It is not known whether ITD and ILD encoding shares a common hemispheric distribution. Using a continuous-stimulus, adapter-probe design, the present study investigated whether ILD changes conform to the response signature of ITD changes, perhaps implicating integration at early cortical structures and a common encoding mechanism.

Behavioral controls were administered to ensure that the relative changes in ITD and ILD were perceived as similar lateralization changes. A comparable relationship was found

between target-probe conditions (see Fig. 3), indicating that the relative ITD and ILD step sizes were perceived at similar intracranial positions for the stimuli tested here (i.e., narrowband, low-frequency noise). Using a more precise lateralization matching paradigm, Edmonds and Krumbholz (2014) found that, on average, a 250-μs ITD matched the perceived lateralization of a 9.3-dB ILD, for low pass-filtered noise below 1 kHz (a somewhat broader stimulus than in the present study). At around 400-μs ITD, they observed matched ILDs around 19 dB, although variability was considerably greater at this more extreme lateralization. Because Edmonds and Krumbholz were concerned with the relationship between single cues and the perceived effect of combining the two cues, it was necessary for a more individualized approach to stimulus parameters; however, the present design investigated the single cues alone and therefore could fix the stimulus parameters across subjects. Nevertheless, the general agreement across studies supports subsequent inferences regarding the measured cortical responses with respect to perceived lateral positions by the tested binaural cues.

The ITD and ILD shifts observed in the present study were shown to elicit robust ERPs that were monotonically greater as the magnitude of the shift increased up to 1,000 μs and 40 dB, respectively (Figs. 4 and 5). This common effect was not unexpected, as others also have reported ERPs to have proportional magnitudes to small and large ITD shifts (Edmonds and Krumbholz 2014; Magezi and Krumbholz 2010; Ozmeral et al. 2016), as well as free-field spatial changes (Briley et al. 2013), abrupt intensity changes (see Ross et al. 1999), and variation to signal level in a background noise (Billings et al. 2009; Whiting et al. 1998). These previous studies of binaural cues, however, have often limited shifts in one spatial hemifield, whereas the present study examined shifts in the two spatial hemifields as well as across hemifields. A sigmoidal model was applied to the GFP at both N1 and P2 latencies (Figs. 4*C* and 5*C*) to determine the relationship between shift magnitude and evoked response. At the N1 latency, the difference between cue type was minimal; however, at the P2 latency, the ILD responses had a noticeably steeper function, indicating continued late-stage processing of ILD changes that were not as evident for ITD shifts. Nevertheless, the main effect of shift magnitude for both cues suggests a common neural weighting scheme to perceived lateralization.

A greater discrepancy in neural signatures arise between responses to ITD and ILD shifts when the effect of shift direction is assessed. The global field potential from the scalp

recordings reproduced previous results for ITDs, in which outward shifts elicited greater responses than inward shifts; however, there was no effect of shift direction on evoked responses to ILD shifts. On further investigation using source-localized activity from a cortical atlas (Destrieux et al. 2010), direction was shown to have an interactive effect with the spatial hemifield for ILD stimuli, whereas ITDs mostly showed a main effect of direction, independent of spatial hemifield (Table 1). Although hemispheric distribution of binaural activity is not necessarily indicative of the mechanism by which these cues are encoded, the clear difference in hemispheric coding of ILD shifts shows the value in assessing the hemispheric activity when the common coding schemes between ITDs and ILDs are investigated. In the present study, ILDs evoked the strongest N1 responses in the right auditory cortex, regardless of the perceived spatial hemifield, whereas ITDs evoked stronger responses in the contralateral hemisphere to the lateralized position. Previous studies have also noted a contralateral effect for both ITDs and ILDs (Krumbholz et al. 2005; McEvoy et al. 1994; Woldorff et al. 1999), although in most cases, stimuli were only presented in the left spatial hemifield, which would have highlighted contralateral effects in the right auditory cortex but would have failed to capture an ipsilateral effect for right hemifield stimuli. In the present study, stimuli were presented in both the left and right hemifields. Right hemisphere bias has also been noted by several studies for auditory-space encoding (Briley et al. 2013; Krumbholz et al. 2005; Magezi and Krumbholz 2010; Schönwiesner et al. 2007; Stecker et al. 2015), but it appears that the method of stimulus presentation can influence which cues show the right hemisphere bias.

With respect to shift direction, an outward-dominant response for ITDs in an adapter-probe stimulus construct has been argued to support a population rate code of auditory space (Magezi and Krumbholz 2010; Salminen et al. 2009, 2010), whereas indistinct responses for shift direction, or even an inward-biased response, have been presented as likely measures of a topographical coding mechanism (Magezi and Krumbholz 2010). Traditionally, these arguments have been considered with respect to ITD coding; however, the basic assumptions can be attributed to ILD coding as well. Despite a number of imaging studies and animal neurophysiology that show evidence for an opponent-channel ILD coding mechanism (McLaughlin et al. 2016; Panniello et al. 2018), the present data are only partially consistent with this view. Whereas early opponent-channel processing (i.e., N1 response) was implicated for ILD coding of stimuli in the left hemifield, the same was not observed when ILD shifted in the right hemifield. Specifically, inward shifts in the right hemifield led to larger responses than for outward shifts in the ipsilateral A1. In addition, inward shifts in the left hemifield evoked stronger P2 responses in the ipsilateral A1, suggesting alternative processing schemes than those observed for ITD stimuli that are not congruent with predictions of an opponent-channel model. One major difference between the present study and studies that have implicated an opponent-channel coding model for ILDs is the stimulus presentation construct. In isolation, or in click trains, binaural stimuli will evoke a graded response that favors the contralateral hemisphere (e.g., Derey et al. 2016; McLaughlin et al. 2016), and this has been the main support for an opponent-channel coding mechanism without necessarily

marking whether activity is due to neurons narrowly tuned to contralaterally lateralized positions or broadly tuned to contralateral spatial hemifields. Only for broadly tuned neural populations would there be a need for an opponent-channel mechanism to infer spatial position. Thus the magnitude of the transition response in an adapter-probe construct as invoked in the present study is best suited for demonstrating whether ITD or ILD coding is based on a population rate rather than a place code, and the present data are consistent with an ITD rate code but appear to deviate from those expectations for ipsilateral ILD shifts. The question remains, if ILDs are not coded in the ipsilateral A1 through an opponent-channel processes, then what other mechanism could be responsible for the observed data? From single and multiunit neural responses to ILD cues, there exists very little evidence supporting a topographical place code for ILD in mammalian auditory cortex (King et al. 2007). Whereas several studies have also had mixed conclusions regarding potential cortical integration of ITD and ILD coding (Altmann et al. 2014; Salminen et al. 2015), in general, most studies do agree that ILDs are broadly tuned in the contralateral A1 (Gutschalk and Steinmann 2015; Palomäki et al. 2005; Stecker et al. 2015). In fact, it is more of a debate as to whether or not ITDs are broadly tuned in the contralateral hemisphere (e.g., Ungan et al. 2001).

In sum, the results of the present study do not fully support the previous supposition that ILDs are encoded by an opponent-channel process. Many of these earlier results were based on observed contralateral activity for static ILDs. Under an adapter-probe construct, as has been previously used to demonstrate opponent-channel processing of ITDs, the present results indicate that the effects of lateral shift direction cannot be explained fully by an opponent-channel model. Moreover, dynamic ILD and ITD shifts were shown to have mostly disparate cortical distributions, consistent with minimal binaural cue integration despite perceptual similarities.

DISCLOSURES

No conflicts of interest, financial or otherwise, are declared by the authors.

AUTHOR CONTRIBUTIONS

E.J.O., D.A.E., and A.C.E. conceived and designed research; E.J.O. performed experiments; E.J.O. analyzed data; E.J.O. interpreted results of experiments; E.J.O. prepared figures; E.J.O. drafted manuscript; E.J.O., D.A.E., and A.C.E. edited and revised manuscript; E.J.O., D.A.E., and A.C.E. approved final version of manuscript.

REFERENCES

Ahveninen J, Kopčo N, Jääskeläinen IP. Psychophysics and neuronal bases of sound localization in humans. *Hear Res* 307: 86–97, 2014. doi:10.1016/j.heares.2013.07.008.

Altmann CF, Terada S, Kashino M, Goto K, Mima T, Fukuyama H, Furukawa S. Independent or integrated processing of interaural time and level differences in human auditory cortex? *Hear Res* 312: 121–127, 2014. doi:10.1016/j.heares.2014.03.009.

ANSI. *ANSI S3.21-2010. Methods for Manual Pure-Tone Threshold Audiometry.* New York: American National Standards Institute, 2010.

Billings CJ, Tremblay KL, Stecker GC, Tolin WM. Human evoked cortical activity to signal-to-noise ratio and absolute signal level. *Hear Res* 254: 15–24, 2009. doi:10.1016/j.heares.2009.04.002.

Blauert J. *Spatial Hearing: The Psychophysics of Human Sound Localization.* Cambridge, MA: MIT Press, 1997.

Briley PM, Kitterick PT, Summerfield AQ. Evidence for opponent process analysis of sound source location in humans. *J Assoc Res Otolaryngol* 14: 83–101, 2013. doi:10.1007/s10162-012-0356-x.

Derey K, Valente G, de Gelder B, Formisano E. Opponent coding of sound location (azimuth) in planum temporale is robust to sound-level variations. *Cereb Cortex* 26: 450–464, 2016. doi:10.1093/cercor/bhv269.

Destrieux C, Fischl B, Dale A, Halgren E. Automatic parcellation of human cortical gyri and sulci using standard anatomical nomenclature. *Neuroimage* 53: 1–15, 2010. doi:10.1016/j.neuroimage.2010.06.010.

Edmonds BA, Krumbholz K. Are interaural time and level differences represented by independent or integrated codes in the human auditory cortex? *J Assoc Res Otolaryngol* 15: 103–114, 2014. doi:10.1007/s10162-013-0421-0.

Gramfort A, Luessi M, Larson E, Engemann DA, Strohmeier D, Brodbeck C, Parkkonen L, Hämäläinen MS. MNE software for processing MEG and EEG data. *Neuroimage* 86: 446–460, 2014. doi:10.1016/j.neuroimage.2013.10.027.

Gramfort A, Papadopoulo T, Olivi E, Clerc M. OpenMEEG: opensource software for quasistatic bioelectromagnetics. *Biomed Eng Online* 9: 45, 2010. doi:10.1186/1475-925X-9-45.

Grech R, Cassar T, Muscat J, Camilleri KP, Fabri SG, Zervakis M, Xanthopoulos P, Sakkalis V, Vanrumste B. Review on solving the inverse problem in EEG source analysis. *J Neuroeng Rehabil* 5: 25, 2008. doi:10.1186/1743-0003-5-25.

Griffiths TD, Büchel C, Frackowiak RS, Patterson RD. Analysis of temporal structure in sound by the human brain. *Nat Neurosci* 1: 422–427, 1998. doi:10.1038/1637.

Griffiths TD, Rees A, Witton C, Cross PM, Shakir RA, Green GG. Spatial and temporal auditory processing deficits following right hemisphere infarction. A psychophysical study. *Brain* 120: 785–794, 1997. doi:10.1093/brain/120.5.785.

Grothe B, Pecka M, McAlpine D. Mechanisms of sound localization in mammals. *Physiol Rev* 90: 983–1012, 2010. doi:10.1152/physrev.00026.2009.

Gutschalk A, Steinmann I. Stimulus dependence of contralateral dominance in human auditory cortex. *Hum Brain Mapp* 36: 883–896, 2015. doi:10.1002/hbm.22673.

Higgins NC, McLaughlin SA, Rinne T, Stecker GC. Evidence for cue-independent spatial representation in the human auditory cortex during active listening. *Proc Natl Acad Sci USA* 114: E7602–E7611, 2017. doi:10.1073/pnas.1707522114.

Holmes CJ, Hoge R, Collins L, Woods R, Toga AW, Evans AC. Enhancement of MR images using registration for signal averaging. *J Comput Assist Tomogr* 22: 324–333, 1998. doi:10.1097/00004728-199803000-00032.

King A, Middlebrooks J. Cortical representation of auditory space. In: *The Auditory Cortex*, edited by Winer JA, Schreiner CE. New York: Springer Science+Business Media, 2010, p. 329–341.

King AJ, Bajo VM, Bizley JK, Campbell RA, Nodal FR, Schulz AL, Schnupp JW. Physiological and behavioral studies of spatial coding in the auditory cortex. *Hear Res* 229: 106–115, 2007. doi:10.1016/j.heares.2007.01.001.

Kohn M, Lifshitz K, Litchfield D. Averaged evoked potentials and frequency modulation. *Electroencephalogr Clin Neurophysiol* 45: 236–243, 1978. doi:10.1016/0013-4694(78)90007-X.

Krumbholz K, Schönwiesner M, von Cramon DY, Rübsamen R, Shah NJ, Zilles K, Fink GR. Representation of interaural temporal information from left and right auditory space in the human planum temporale and inferior parietal lobe. *Cereb Cortex* 15: 317–324, 2005. doi:10.1093/cercor/bhh133.

Kybic J, Clerc M, Abboud T, Faugeras O, Keriven R, Papadopoulo T. A common formalism for the integral formulations of the forward EEG problem. *IEEE Trans Med Imaging* 24: 12–28, 2005. doi:10.1109/TMI.2004.837363.

Luck SJ. *An Introduction to the Event-Related Potential Technique*. Cambridge, MA: MIT Press, 2014.

Magezi DA, Krumbholz K. Evidence for opponent-channel coding of interaural time differences in human auditory cortex. *J Neurophysiol* 104: 1997–2007, 2010. doi:10.1152/jn.00424.2009.

McEvoy L, Mäkelä JP, Hämäläinen M, Hari R. Effect of interaural time differences on middle-latency and late auditory evoked magnetic fields. *Hear Res* 78: 249–257, 1994. doi:10.1016/0378-5955(94)90031-0.

McEvoy LK, Picton TW, Champagne SC, Kellett AJ, Kelly JB. Human evoked potentials to shifts in the lateralization of a noise. *Audiology* 29: 163–180, 1990. doi:10.3109/00206099009072848.

McLaughlin SA, Higgins NC, Stecker GC. Tuning to binaural cues in human auditory cortex. *J Assoc Res Otolaryngol* 17: 37–53, 2016. doi:10.1007/s10162-015-0546-4.

Nasreddine ZS, Phillips NA, Bédirian V, Charbonneau S, Whitehead V, Collin I, Cummings JL, Chertkow H. The Montreal Cognitive Assessment, MoCA: a brief screening tool for mild cognitive impairment. *J Am Geriatr Soc* 53: 695–699, 2005. doi:10.1111/j.1532-5415.2005.53221.x.

Ozmeral EJ, Eddins DA, Eddins AC. Reduced temporal processing in older, normal-hearing listeners evident from electrophysiological responses to shifts in interaural time difference. *J Neurophysiol* 116: 2720–2729, 2016. doi:10.1152/jn.00560.2016.

Palomäki KJ, Tiitinen H, Mäkinen V, May PJ, Alku P. Spatial processing in human auditory cortex: the effects of 3D, ITD, and ILD stimulation techniques. *Brain Res Cogn Brain Res* 24: 364–379, 2005. doi:10.1016/j.cogbrainres.2005.02.013.

Panniello M, King AJ, Dahmen JC, Walker KM. Local and global spatial organization of interaural level difference and frequency preferences in auditory cortex. *Cereb Cortex* 28: 350–369, 2018. doi:10.1093/cercor/bhx295.

Pascual-Marqui RD. Standardized low-resolution brain electromagnetic tomography (sLORETA): technical details. *Methods Find Exp Clin Pharmacol* 24, Suppl D: 5–12, 2002.

Picton TW, Woods DL, Baribeau-Braun J, Healey TM. Evoked potential audiometry. *J Otolaryngol* 6: 90–119, 1976.

Riedel H, Kollmeier B. Auditory brain stem responses evoked by lateralized clicks: is lateralization extracted in the human brain stem? *Hear Res* 163: 12–26, 2002. doi:10.1016/S0378-5955(01)00362-8.

Ross B, Lütkenhöner B, Pantev C, Hoke M. Frequency-specific threshold determination with the CERAgram method: basic principle and retrospective evaluation of data. *Audiol Neurotol* 4: 12–27, 1999. doi:10.1159/000013816.

Salminen NH, May PJ, Alku P, Tiitinen H. A population rate code of auditory space in the human cortex. *PLoS One* 4: e7600, 2009. doi:10.1371/journal.pone.0007600.

Salminen NH, Takanen M, Santala O, Lamminsalo J, Altoè A, Pulkki V. Integrated processing of spatial cues in human auditory cortex. *Hear Res* 327: 143–152, 2015. doi:10.1016/j.heares.2015.06.006.

Salminen NH, Tiitinen H, Yrttiaho S, May PJ. The neural code for interaural time difference in human auditory cortex. *J Acoust Soc Am* 127: EL60–EL65, 2010. doi:10.1121/1.3290744.

Schönwiesner M, Krumbholz K, Rübsamen R, Fink GR, von Cramon DY. Hemispheric asymmetry for auditory processing in the human auditory brain stem, thalamus, and cortex. *Cereb Cortex* 17: 492–499, 2007. doi:10.1093/cercor/bhj165.

Schröger E. Interaural time and level differences: integrated or separated processing? *Hear Res* 96: 191–198, 1996. doi:10.1016/0378-5955(96)00066-4.

Skrandies W. Global field power and topographic similarity. *Brain Topogr* 3: 137–141, 1990. doi:10.1007/BF01128870.

Stecker GC. Temporal binding of auditory spatial information across dynamic binaural events. *Atten Percept Psychophys* 80: 14–20, 2018. doi:10.3758/s13414-017-1436-0.

Stecker GC, McLaughlin SA, Higgins NC. Monaural and binaural contributions to interaural-level-difference sensitivity in human auditory cortex. *Neuroimage* 120: 456–466, 2015. doi:10.1016/j.neuroimage.2015.07.007.

Tadel F, Baillet S, Mosher JC, Pantazis D, Leahy RM. Brainstorm: a user-friendly application for MEG/EEG analysis. *Comput Intell Neurosci* 2011: 879716, 2011. doi:10.1155/2011/879716.

Tardif E, Murray MM, Meylan R, Spierer L, Clarke S. The spatio-temporal brain dynamics of processing and integrating sound localization cues in humans. *Brain Res* 1092: 161–176, 2006. doi:10.1016/j.brainres.2006.03.095.

Ungan P, Yagcioglu S, Goksoy C. Differences between the N1 waves of the responses to interaural time and intensity disparities: scalp topography and dipole sources. *Clin Neurophysiol* 112: 485–498, 2001. doi:10.1016/S1388-2457(00)00550-2.

Uusitalo MA, Ilmoniemi RJ. Signal-space projection method for separating MEG or EEG into components. *Med Biol Eng Comput* 35: 135–140, 1997. doi:10.1007/BF02534144.

von Kriegstein K, Griffiths TD, Thompson SK, McAlpine D. Responses to interaural time delay in human cortex. *J Neurophysiol* 100: 2712–2718, 2008. doi:10.1152/jn.90210.2008.

Werner-Reiss U, Groh JM. A rate code for sound azimuth in monkey auditory cortex: implications for human neuroimaging studies. *J Neurosci* 28: 3747–3758, 2008. doi:10.1523/JNEUROSCI.5044-07.2008.

Whiting KA, Martin BA, Stapells DR. The effects of broadband noise masking on cortical event-related potentials to speech sounds /ba/ and /da/. *Ear Hear* 19: 218–231, 1998. doi:10.1097/00003446-199806000-00005.

Woldorff MG, Tempelmann C, Fell J, Tegeler C, Gaschler-Markefski B, Hinrichs H, Heinz HJ, Scheich H. Lateralized auditory spatial perception and the contralaterality of cortical processing as studied with functional magnetic resonance imaging and magnetoencephalography. *Hum Brain Mapp* 7: 49–66, 1999. doi:10.1002/(SICI)1097-0193(1999)7:1<49:AID-HBM5>3.0.CO;2-J.

Zatorre RJ, Bouffard M, Ahad P, Belin P. Where is 'where' in the human auditory cortex? *Nat Neurosci* 5: 905–909, 2002. doi:10.1038/nn904.

Zatorre RJ, Mondor TA, Evans AC. Auditory attention to space and frequency activates similar cerebral systems. *Neuroimage* 10: 544–554, 1999. doi:10.1006/nimg.1999.0491.

Zatorre RJ, Penhune VB. Spatial localization after excision of human auditory cortex. *J Neurosci* 21: 6321–6328, 2001. doi:10.1523/JNEUROSCI.21-16-06321.2001.